Progress In Electromagnetics Research C, Vol. 108, 89–101, 2021

Joint Beamforming and Phase Shifts Design in Double Intelligent Reflect Surface Aided Secrecy MISO Channel

Jun Shao* **and Jinxin Zhu**

Abstract—In this paper, we study a double intelligent reflect surface (IRS) aided secrecy transmission design in multiple-input single-output (MISO) channel. Specifically, we investigate a joint active and passive beamforming design to maximize the secrecy rate, subject to multiple non-convex constraints. An alternating optimization (AO) method is proposed, where the unit modulus constraints are handled by the alternating direction of multipliers method (ADMM) and majorization-minimization (MM) methods. Simulation results show the superiority of the proposed design.

1. INTRODUCTION

Recently, smart antenna technique has drawn great attention in industry and academia [1–3]. Specifically, in [1], the authors presented the results of the synthesis of a light-weight inexpensive reconfigurable planar array antenna. In [2], a microstrip antenna array prototype composed by four elements was fabricated and experimentally tested. In [3], the authors investigated the design of forward-looking mono-pulse arrays able to reconfigure the radiation pattern.

On the other hand, with the rapid development of radio frequency (RF) micro electro-mechanical systems, programmable and reconfigurable meta-surfaces have found abundant applications, among which intelligent reflecting surface (IRS) has drawn special attention for its applications in wireless communications [4]. IRS is a cost-effective device composed of a large number of reflecting elements, each of which can reflect electromagnetic waves with adjusted phase shifts [5]. Furthermore, different from the conventional transceivers, IRS helps transmit information without generating new signals [6]. Thus, IRS can be seen as a no-power full-duplex (FD) amplify-and-forward (AF) relay to provide a new link in the dead zones [7]. Compared with the common FD AF relay, IRS consumes almost no energy, and thus it has higher energy efficiency than regular FD AF relay [8].

Due to these significant merits, IRS has attracted great research interest in various communication systems [9]. Specifically, in [10], the authors investigated the passive beamforming (BF) design in an IRS aided multiple-input single-output (MISO) network. In [11], the authors investigated the weighted sum-rate optimization for IRS aided multiuser wireless networks. In addition, IRS-aided transmission has been investigated with several new techniques such as the millimeter-wave communication, cognitive radio (CR), simultaneous wireless information and power transfer (SWIPT), unmanned aerial vehicle (UAV) communication, and machine learning in [12–16], respectively.

On the other hand, physical layer security (PLS) has been thoroughly investigated as a complement to higher layer encryption techniques, to ensure communication security from the information-theoretic perspective [17]. By exploiting the spatial degrees of freedom (DoF), the transmission BF can be designed to direct the signal towards the legitimate user (Bob) and meanwhile degrade the reception at the eavesdropper (Eve), so that the secrecy performance can be improved [18]. Since IRS can enhance or weaken the signal strength at different receivers, it is beneficial to PLS design [19].

Received 27 October 2020, Accepted 28 December 2020, Scheduled 6 January 2021
* Corresponding author: Jun Shao (sj@ycit.edu.cn).
The authors are with the School of Information Technology, Yancheng Institute of Technology, Yancheng 224051, China.

Recently, several works have investigated the applications of IRS in PLS. Specifically, for the MISO wiretap channel, in [20] and [21], the authors investigated the IRS assisted secrecy communication without and with considering artificial noise (AN), respectively. In [22], the authors investigated the IRS assisted secure transmission without Eve's channel state information (CSI). Furthermore, for a multiple-input multiple-output (MIMO) wiretap channel, in [23] and [24], the authors investigated the IRS aided secure transmission using the one by one optimization and majorization-minimization (MM) method, respectively. Both works did not consider AN. In [25], the authors investigated an IRS assisted secure precoding and AN design, where a block coordinate descent (BCD) and MM based method was proposed. Recently in [26], the authors investigated the IRS-aided secrecy MIMO communication with wireless energy harvesting, where a penalty based method was proposed. Furthermore, the robust design in IRS-aided secrecy communication has been investigated in [27] and [28] without and with cooperative jammer, respectively.

Commonly, current research on IRS mainly focuses on the joint BF design, which only studies the scenario with one IRS or multiple faraway IRSs with each independently serving its associated users in the vicinity. To further improve the performance, in [29], the authors investigated a BF design in a double IRS aided MISO channel, where a power scaling has been proposed. In [30], the authors investigated joint channel estimation and BF design in a double IRS aided MIMO channel, which suggests that double IRSs can achieve better performance than a single IRS. Recently in [31], the authors investigated a multi-user cooperative BF design in a double IRS aided MIMO channel.

However, these works were not security concerned. In fact, in a security concerned scenario, the design problem is commonly hard to handle due to the non-convex secrecy rate expression and the unit modulus constraint (UMC) of the IRS, while the cascaded multiple IRSs scenario makes the problem even harder. Motivated by this, in this work, we investigate a double IRS aided PLS design in a MISO wiretap channel. Specifically, we aim to maximize the secrecy rate by jointly designing the passive BF and active BF, with considering both continuous reflecting coefficient (RC) and discrete RC. The formulated problem is hard to handle mainly due to the non-convex UMC. To overcome this obstacle, we propose an alternating optimization (AO) method, where the UMC is handled by the alternating direction of multipliers method (ADMM) and MM methods, with the advantages of better secrecy rate performance and lower computational complexity, respectively. Moreover, since each subproblem has the corresponding solution in a closed from, the entire AO method can be proceeded conveniently and efficiently without using any convex optimization tool. In addition, the proposed method can be extended to the multiple IRSs case directly. Simulation results verify the performance of the proposed method.

The rest of this paper is organized as follows. A system model description and problem statement are given in Section 2. Section 3 investigates the joint BF design, where an AO approach is established. Section 4 investigates the extension of the proposed method. Simulation results are illustrated in Section 5. Section 6 concludes this paper.

Notations: Throughout this paper, boldface lowercase and uppercase letters denote vectors and matrices, respectively. The transpose, conjugate, conjugate transpose, trace of matrix $\mathbf{A}$ are denoted as $\mathbf{A}^T$, $\mathbf{A}^\dagger$, $\mathbf{A}^H$, and $\mathrm{Tr}\,(\mathbf{A})$, respectively. $\mathbf{A} \succeq \mathbf{0}$ indicates that $\mathbf{A}$ is a positive semi-definite matrix. $\mathbf{I}$ is an identity matrix with proper dimension. $\mathcal{CN}(\mathbf{0}, \mathbf{I})$ denotes a circularly symmetric complex Gaussian random vector with mean $\mathbf{0}$ and covariance $\mathbf{I}$. $\angle$ means to extract the angle of a complex.

2. SYSTEM MODEL AND PROBLEM STATEMENT

2.1. System Model

As shown in Fig. 1, we consider a downlink MISO system which consists of one BS, two IRSs, one Bob, and one Eve. We focus on a challenging scenario where the BS-Bob/Eve/IRS2 links and IRS1-Bob/Eve links are blocked by obstacles. To enhance the communication, we place IRS1 near the BS, and IRS2 near the Bob, such that the Bob can be served by the BS through the double reflection link, i.e., the BS-IRS1-IRS2-Bob link. Besides, there exists an Eve near the Bob, who can eavesdrop the confidential information through the double reflection link, i.e., the BS-IRS1-IRS2-Eve link. Besides, we assume that the BS and two IRSs are equipped with N_t antennas and M_1, M_2 reflecting elements, respectively, while the Bob and Eve are both equipped with single antenna. We denote $\mathbf{F} \in \mathbb{C}^{M_1 \times N_t}$, $\mathbf{D} \in \mathbb{C}^{M_2 \times M_1}$,

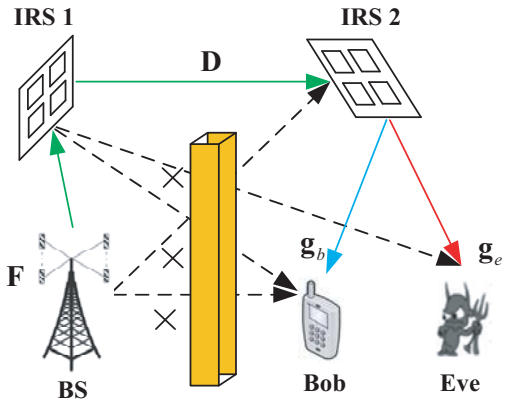

Figure 1. The double IRS-aided secure MISO system model.

$\mathbf{g}_b \in \mathbb{C}^{M_2 \times 1}$ and $\mathbf{g}_e \in \mathbb{C}^{M_2 \times 1}$ as the channels from BS to IRS1, from IRS1 to IRS2, from IRS2 to Bob, and from IRS2 to Eve, respectively. In addition, it should be noted that since the power of signals reflected two or more times is much smaller than that of the signal reflected only one time, we only consider one time reflection in this work.

The BS uses BF vector $\mathbf{w}$ to transmit the confidential message s to Bob with the aid of the two IRSs. Without loss of generality (W.l.o.g.), we assume that $\mathbb{E}\{|s|^2\} = 1$. Thus, the received signals at the Bob and Eve are, respectively, given by

$$y_b = \mathbf{g}_b^H \mathbf{\Phi}_2^H \mathbf{D} \mathbf{\Phi}_1^H \mathbf{F} \mathbf{w} s + n_b, \tag{1a}$$

$$y_e = \mathbf{g}_e^H \mathbf{\Phi}_2^H \mathbf{D} \mathbf{\Phi}_1^H \mathbf{F} \mathbf{w} s + n_e, \tag{1b}$$

where $\mathbf{\Phi}_1$ and $\mathbf{\Phi}_2$ denote the RC at the IRS1 and IRS2, respectively, and n_b and n_e are the zero-mean additive white Gaussian noises at the Bob and Eve, with variances σ_b^2 and σ_e^2, respectively.

2.2. Reflecting Coefficient Model

In this subsection, we discuss the RC model. Let us denote $\theta_m, m \in \mathcal{M} = \{1, \ldots, M\}$ as the RC of the m-th reflection element. The phase-shift matrix of the IRS is denoted by a diagonal matrix $\mathbf{\Phi} = \sqrt{\eta}\text{diag}(\theta_1, \ldots, \theta_M)$ (where $\eta \leq 1$ indicates the reflection efficiency, w.l.o.g., we assume that $\eta = 1$ in the work).

The first RC model is the continuous RC model, in which only the phase of the received signal is changed, while the strength of the reflection signal from each reflection element is maximized, i.e., $|\theta_m| = 1$. Since θ_m can be optimized to any possible phase, we have:

$$\mathcal{F}_1 = \left\{ \theta_m | \theta_m = e^{j\phi_m}, \phi_m \in [0, 2\pi) \right\}. \tag{2}$$

The second RC model is the discrete RC case, i.e., the reflection element only takes finite values. Similar to [8], we assume that θ_m has τ discrete values, which are equally spaced on the circle, i.e.,

$$\mathcal{F}_2 = \left\{ \theta_m | \theta_m = e^{j\phi_m}, \phi_m \in \left\{ 0, \frac{2\pi}{\tau}, \ldots, \frac{2\pi(\tau-1)}{\tau} \right\} \right\}. \tag{3}$$

2.3. Problem Statement

In this work, we aim to maximize the secrecy rate by jointly design the active BF and the phase shifters. Mathematically, the problem is given as

$$\max_{\mathbf{w}, \mathbf{\Phi}_1, \mathbf{\Phi}_2} \quad \frac{1 + \frac{\left| \mathbf{g}_b^H \mathbf{\Phi}_2^H \mathbf{D} \mathbf{\Phi}_1^H \mathbf{F} \mathbf{w} \right|^2}{\sigma_b^2}}{1 + \frac{\left| \mathbf{g}_e^H \mathbf{\Phi}_2^H \mathbf{D} \mathbf{\Phi}_1^H \mathbf{F} \mathbf{w} \right|^2}{\sigma_e^2}} \tag{4a}$$

$$\text{s.t.} \qquad \|\mathbf{w}\|^2 \le P_s, \tag{4b}$$

$$|\mathbf{\Phi}_i| \in \mathcal{F}_1 \; or \; |\mathbf{\Phi}_i| \in \mathcal{F}_2, i = 1, 2, \tag{4c}$$

where P_s denotes the total power budget at the BS.

The formulate joint active BF and phase shifters design is hard to tackle, mainly due to the coupled variables and the UMC. Since the method utilized in the continuous RC case can be used to the discrete RC case directly, we will focus on the continuous RC case in the following part.

3. THE JOINT ACTIVE AND PASSIVE BF DESIGN

In this section, we decouple Eq. (4) into several subproblems and then propose an AO method, where each subproblem can be solved efficiently.

3.1. The Optimization of the Active BF

First, we assume that parameters $\mathbf{\Phi}_1$ and $\mathbf{\Phi}_2$ are fixed and derive the optimal value of $\mathbf{w}$. To this end, the objective function in problem of Eq. (4) is reformulated, and then considering that the log function is monotonically increasing, it is removed. Therefore, the following problem is formulated

$$\max_{\mathbf{w}} \qquad \frac{\left|\mathbf{g}_b^H \mathbf{\Phi}_2^H \mathbf{D} \mathbf{\Phi}_1^H \mathbf{F} \mathbf{w}\right|^2 + \sigma_b^2}{\left|\mathbf{g}_e^H \mathbf{\Phi}_2^H \mathbf{D} \mathbf{\Phi}_1^H \mathbf{F} \mathbf{w}\right|^2 + \sigma_e^2} \tag{5a}$$

$$\text{s.t.} \qquad \|\mathbf{w}\|^2 \le P_s. \tag{5b}$$

From the conclusion in [12], the optimal $\mathbf{w}$ is $\mathbf{w}^\star = \sqrt{P_s}\mathbf{v}_{\max}(\mathbf{A}, \mathbf{B})$, where $\mathbf{v}_{\max}$ is the normalized eigenvector corresponding to the largest eigenvalue of the matrix pair $(\mathbf{A}, \mathbf{B})$, while $\mathbf{A}$ and $\mathbf{B}$ are, respectively, given as

$$\mathbf{A} = \frac{1}{\sigma_b^2} \mathbf{g}_b^H \mathbf{\Phi}_2^H \mathbf{D} \mathbf{\Phi}_1^H \mathbf{F} \left(\mathbf{g}_b^H \mathbf{\Phi}_2^H \mathbf{D} \mathbf{\Phi}_1^H \mathbf{F}\right)^H + \frac{\mathbf{I}}{P_s}, \tag{6a}$$

$$\mathbf{B} = \frac{1}{\sigma_e^2} \mathbf{g}_e^H \mathbf{\Phi}_2^H \mathbf{D} \mathbf{\Phi}_1^H \mathbf{F} \left(\mathbf{g}_e^H \mathbf{\Phi}_2^H \mathbf{D} \mathbf{\Phi}_1^H \mathbf{F}\right)^H + \frac{\mathbf{I}}{P_s}. \tag{6b}$$

3.2. The Optimization of the Passive BF Using the ADMM Method

In this subsection, we will handle the subproblem with respect to (w.r.t.) the phase shift. In fact, due to the symmetry of $\mathbf{\Phi}_1$ and $\mathbf{\Phi}_2$ in Eq. (4a), the method used to optimize $\mathbf{\Phi}_1$ can be used to optimize $\mathbf{\Phi}_2$ directly. Thus, in the following, we will fucus on the optimization of $\mathbf{\Phi}_1$. Firstly, we introduce the following lemma.

Lemma 1 [14]: Let $\mathbf{C}_1 \in \mathbb{C}^{m \times m}$ and $\mathbf{C}_2 \in \mathbb{C}^{m \times m}$ be matrices, and $\mathbf{1} = [1, \ldots, 1]^T$ is a $m \times 1$ vector. Assuming that $\mathbf{E} \in \mathbb{C}^{m \times m}$ is a diagonal matrix $\mathbf{E} = \text{diag}(e_1, \ldots, e_2)$, and $\mathbf{e} = \mathbf{E}\mathbf{1}$, then the following matrix identity holds:

$$\text{Tr}\left(\mathbf{E}^H \mathbf{C}_1 \mathbf{E} \mathbf{C}_2\right) = \mathbf{e}^H \left(\mathbf{C}_1 \odot \mathbf{C}_2^T\right) \mathbf{e}. \tag{7}$$

Via Lemma 1, the terms $|\mathbf{g}_b^H \mathbf{\Phi}_2^H \mathbf{D} \mathbf{\Phi}_1^H \mathbf{F} \mathbf{w}|^2$ and $|\mathbf{g}_e^H \mathbf{\Phi}_2^H \mathbf{D} \mathbf{\Phi}_1^H \mathbf{F} \mathbf{w}|^2$ can be rewritten as

$$\begin{aligned} \left|\mathbf{g}_b^H \mathbf{\Phi}_2^H \mathbf{D} \mathbf{\Phi}_1^H \mathbf{F} \mathbf{w}\right|^2 &= \text{Tr}\left(\mathbf{\Phi}_1^H \mathbf{F} \mathbf{W} \mathbf{F}^H \mathbf{\Phi}_1 \mathbf{D}^H \mathbf{\Phi}_2 \mathbf{g}_b \mathbf{g}_b^H \mathbf{\Phi}_2^H \mathbf{D}\right) \\ &= \boldsymbol{\theta}_1^H \left(\mathbf{F} \mathbf{W} \mathbf{F}^H \odot \left(\mathbf{D}^H \mathbf{\Phi}_2 \mathbf{g}_b \mathbf{g}_b^H \mathbf{\Phi}_2^H \mathbf{D}\right)^T\right) \boldsymbol{\theta}_1, \end{aligned} \tag{8a}$$

$$\begin{aligned} \left|\mathbf{g}_e^H \mathbf{\Phi}_2^H \mathbf{D} \mathbf{\Phi}_1^H \mathbf{F} \mathbf{w}\right|^2 &= \text{Tr}\left(\mathbf{\Phi}_1^H \mathbf{F} \mathbf{W} \mathbf{F}^H \mathbf{\Phi}_1 \mathbf{D}^H \mathbf{\Phi}_2 \mathbf{g}_e \mathbf{g}_e^H \mathbf{\Phi}_2^H \mathbf{D}\right) \\ &= \boldsymbol{\theta}_1^H \left(\mathbf{F} \mathbf{W} \mathbf{F}^H \odot \left(\mathbf{D}^H \mathbf{\Phi}_2 \mathbf{g}_e \mathbf{g}_e^H \mathbf{\Phi}_2^H \mathbf{D}\right)^T\right) \boldsymbol{\theta}_1, \end{aligned} \tag{8b}$$

where $\boldsymbol{\theta}_1 = (\theta_1, \ldots, \theta_{M_1})^T$.

By defining $\mathbf{V}_1 = \mathbf{F}\mathbf{W}\mathbf{F}^H \odot (\mathbf{D}^H \boldsymbol{\Phi}_2 \mathbf{g}_b \mathbf{g}_b^H \boldsymbol{\Phi}_2^H \mathbf{D})^T + \sigma_b^2 \mathbf{I}$, and $\mathbf{V}_2 = \mathbf{F}\mathbf{W}\mathbf{F}^H \odot (\mathbf{D}^H \boldsymbol{\Phi}_2 \mathbf{g}_e \mathbf{g}_e^H \boldsymbol{\Phi}_2^H \mathbf{D})^T + \sigma_e^2 \mathbf{I}$, we obtain the following problem

$$\min \quad \frac{\boldsymbol{\theta}_1^H \mathbf{V}_2 \boldsymbol{\theta}_1}{\boldsymbol{\theta}_1^H \mathbf{V}_1 \boldsymbol{\theta}_1} \tag{9a}$$

$$\text{s.t.} \quad |\boldsymbol{\theta}_1|_m = 1. \tag{9b}$$

The UMC in Eq. (9b) makes Eq. (9) become a general NP-hard quadratic program. To tackle this challenging problem, we simplify the UMC by introducing the auxiliary variables $\boldsymbol{\phi}$ such that Eq. (9) is converted into the following optimization problem without the modulus operation:

$$\min \quad \frac{\boldsymbol{\theta}_1^H \mathbf{V}_2 \boldsymbol{\theta}_1}{\boldsymbol{\theta}_1^H \mathbf{V}_1 \boldsymbol{\theta}_1} \tag{10a}$$

$$\text{s.t.} \quad \boldsymbol{\theta}_1 = e^{j\boldsymbol{\phi}}. \tag{10b}$$

The augmented lagrange function of Eq. (10) is given as follows [32]

$$\mathcal{L}(\boldsymbol{\theta}_1, \boldsymbol{\phi}, \mathbf{r}) = \frac{\boldsymbol{\theta}_1^H \mathbf{V}_2 \boldsymbol{\theta}_1}{\boldsymbol{\theta}_1^H \mathbf{V}_1 \boldsymbol{\theta}_1} + \frac{\alpha}{2}\left(\left\|\boldsymbol{\theta}_1 - e^{j\boldsymbol{\phi}} + \mathbf{r}\right\|^2 - \|\mathbf{r}\|^2\right), \tag{11}$$

where $\alpha > 0$ is the penalty factor, and $\mathbf{r} \in \mathbb{C}^{M_1 \times 1}$ is the scalar dual variable, respectively.

Then, the following iterative steps derived from the ADMM in Eq. (11) are applied to solve Eq. (10)

$$\boldsymbol{\phi}^{n+1} = \arg\min_{\boldsymbol{\phi}} \mathcal{L}(\boldsymbol{\theta}_1^n, \boldsymbol{\phi}^n, \mathbf{r}^n), \tag{12a}$$

$$\boldsymbol{\theta}_1^{n+1} = \arg\min_{\boldsymbol{\theta}_1} \mathcal{L}(\boldsymbol{\theta}_1^n, \boldsymbol{\phi}^{n+1}, \mathbf{r}^n), \tag{12b}$$

$$\mathbf{r}^{n+1} = \mathbf{r}^n + \boldsymbol{\theta}_1^{n+1} - e^{j\boldsymbol{\phi}^{n+1}}, \tag{12c}$$

for $n = 1, \ldots$ until certain stop criterion is meet.

In fact, the main merit of the ADMM method is that each subproblem has a closed-form solution. Specifically, Eq.(12a) is reduced to

$$\min_{\boldsymbol{\phi}} \left\|\boldsymbol{\theta}_1^n - e^{j\boldsymbol{\phi}} + \mathbf{r}^n\right\|^2, \tag{13}$$

and the solution is

$$\boldsymbol{\phi}^{n+1} = \angle(\boldsymbol{\theta}_1^n + \mathbf{r}^n). \tag{14}$$

For Eq. (12b), by the first order condition, we have

$$\frac{2\mathbf{V}_2\boldsymbol{\theta}_1^{n+1}}{(\boldsymbol{\theta}_1^n)^H \mathbf{V}_1 \boldsymbol{\theta}_1^n} - \frac{2(\boldsymbol{\theta}_1^n)^H \mathbf{V}_2 \boldsymbol{\theta}_1^n \mathbf{V}_1 \boldsymbol{\theta}_1^{n+1}}{\left((\boldsymbol{\theta}_1^n)^H \mathbf{V}_1 \boldsymbol{\theta}_1^n\right)^2} + \alpha\left(\boldsymbol{\theta}_1^{n+1} - e^{j\boldsymbol{\phi}^{n+1}} + \mathbf{r}^n\right) = 0, \tag{15}$$

and rearranging Eq. (15), we get

$$\left(\frac{2\mathbf{V}_2}{(\boldsymbol{\theta}_1^n)^H \mathbf{V}_1 \boldsymbol{\theta}_1^n} - \frac{2\mathbf{V}_1(\boldsymbol{\theta}_1^n)^H \mathbf{V}_2 \boldsymbol{\theta}_1^n}{\left((\boldsymbol{\theta}_1^n)^H \mathbf{V}_1 \boldsymbol{\theta}_1^n\right)^2} + \alpha\mathbf{I}\right)\boldsymbol{\theta}_1^{n+1} = \alpha\left(e^{j\boldsymbol{\phi}^{n+1}} - \mathbf{r}^n\right). \tag{16}$$

Thus, the optimal $\boldsymbol{\theta}_1^{n+1}$ is

$$\boldsymbol{\theta}_1^{n+1} = \alpha\left(\frac{2\mathbf{V}_2}{(\boldsymbol{\theta}_1^n)^H \mathbf{V}_1 \boldsymbol{\theta}_1^n} - \frac{2\mathbf{V}_1(\boldsymbol{\theta}_1^n)^H \mathbf{V}_2 \boldsymbol{\theta}_1^n}{\left((\boldsymbol{\theta}_1^n)^H \mathbf{V}_1 \boldsymbol{\theta}_1^n\right)^2} + \alpha\mathbf{I}\right)^{-1}\left(e^{j\boldsymbol{\phi}^{n+1}} - \mathbf{r}^n\right). \tag{17}$$

The entire ADMM procedure is summarized in Algorithm 1, where $(\boldsymbol{\theta}_1^n, \boldsymbol{\phi}^n, \mathbf{r}^n)$ is the obtained optimal solution in the n-th iteration.

Algorithm 1 : The ADMM algorithm for problem in Eq. (9).

1: Initialize with a feasible primal-dual point $(\boldsymbol{\theta}_1^0, \boldsymbol{\phi}^0, \mathbf{r}^0)$, choose $\alpha > 0$ and set $n = 0$.
2: **repeat**
[a)]
(i) Calculate $\boldsymbol{\phi}^{n+1}$ with given $\boldsymbol{\theta}_1^n$ and $\mathbf{r}^n$ by Eq. (14).
(ii) Calculate $\boldsymbol{\theta}_1^{n+1}$ with given $\boldsymbol{\phi}^{n+1}$ and $\mathbf{r}^n$ by Eq. (17).
(iii) Calculate $\mathbf{r}^{n+1}$ with given $\boldsymbol{\theta}_1^{n+1}$ and $\boldsymbol{\phi}_1^{n+1}$ by Eq. (12c).
(iv) $n \leftarrow n + 1$.
3: **until** the stopping criterion is satisfied.
4: **Output** $(\boldsymbol{\theta}_1^\star, \boldsymbol{\phi}^\star, \mathbf{r}^\star)$.

3.3. The Optimization of the Passive BF Using the MM Method

In the following, we will propose an MM method to obtain the phase shift, with lower complexity.

The main idea of the MM method is to solve a difficult problem by constructing a series of more tractable approximated problems. In particular, assuming that the value of $\boldsymbol{\theta}_1$ in the n-th iteration of the MM method is denoted as $\boldsymbol{\theta}_1^n$, we construct a lower bound on the objective function $g(\boldsymbol{\theta}_1)$ that touches the objective function at point $\boldsymbol{\theta}_1^n$, denoted as $f(\boldsymbol{\theta}_1|\boldsymbol{\theta}_1^n)$. We adopt this lower bound as a surrogate objective function, and the maximizer of this surrogate objective function is then taken as the value of $\boldsymbol{\theta}_1$ in the next iteration of the MM procedure, i.e., $\boldsymbol{\theta}_1^{n+1}$. In this way, the objective value monotonically increases from one iteration to the next, i.e., $g(\boldsymbol{\theta}_1^{n+1}) \geq g(\boldsymbol{\theta}_1^n)$. The key to the MM method lies in constructing a surrogate objective function $f(\boldsymbol{\theta}_1|\boldsymbol{\theta}_1^n)$ for which the maximizer $\boldsymbol{\theta}_1^{n+1}$ is easy to find. For the phase shift optimization in Eq. (9), a surrogate objective function is composed in the following lemma.

Lemma 2: The objective function $g(\boldsymbol{\theta}_1)$ can be lower bounded by

$$g(\boldsymbol{\theta}_1) = \frac{\boldsymbol{\theta}_1^H \mathbf{V}_1 \boldsymbol{\theta}_1}{\boldsymbol{\theta}_1^H \mathbf{V}_2 \boldsymbol{\theta}_1} \geq f\left(\boldsymbol{\theta}_1 \left| \boldsymbol{\theta}_1^n \right.\right) + \left[g\left(\boldsymbol{\theta}_1\right) - f\left(\boldsymbol{\theta}_1^n \left| \boldsymbol{\theta}_1^n \right.\right)\right], \tag{18}$$

where

$$\begin{aligned} f\left(\boldsymbol{\theta}_1 \left| \boldsymbol{\theta}_1^n \right.\right) \;=\; & 2\frac{\Re\left\{\left(\boldsymbol{\theta}_1^n\right)^H \mathbf{V}_1 \boldsymbol{\theta}_1\right\}}{\left(\boldsymbol{\theta}_1^n\right)^H \mathbf{V}_2 \boldsymbol{\theta}_1^n} \\ & - \frac{\left(\boldsymbol{\theta}_1^n\right)^H \mathbf{V}_1 \boldsymbol{\theta}_1^n}{\left(\left(\boldsymbol{\theta}_1^n\right)^H \mathbf{V}_2 \boldsymbol{\theta}_1^n\right)^2} \left(\boldsymbol{\theta}_1^H \lambda_{\max}\left(\mathbf{V}_2\right) \boldsymbol{\theta}_1 + 2\Re\left\{\left(\boldsymbol{\theta}_1^n\right)^H \left(\mathbf{V}_2 - \lambda_{\max}\left(\mathbf{V}_2\right) \mathbf{I}\right) \boldsymbol{\theta}_1\right\}\right), \end{aligned} \tag{19}$$

and $g(\boldsymbol{\theta}_1) - f(\boldsymbol{\theta}_1^n|\boldsymbol{\theta}_1^n)$ is a constant term which is irrelevant for optimization.

Proof: Defining $y = \boldsymbol{\theta}_1^H \mathbf{V}_2 \boldsymbol{\theta}_1$, the objective function $\frac{\boldsymbol{\theta}_1^H \mathbf{V}_1 \boldsymbol{\theta}_1}{y}$ is jointly convex in $\{\boldsymbol{\theta}_1, y\}$, since $\mathbf{V}_1$ is positive definite. Due to the convexity, we have the following inequality

$$\frac{\boldsymbol{\theta}_1^H \mathbf{V}_1 \boldsymbol{\theta}_1}{\boldsymbol{\theta}_1^H \mathbf{V}_2 \boldsymbol{\theta}_1} \geq 2\frac{\Re\left\{\left(\boldsymbol{\theta}_1^n\right)^H \mathbf{V}_1 \boldsymbol{\theta}_1\right\}}{\left(\boldsymbol{\theta}_1^n\right)^H \mathbf{V}_2 \boldsymbol{\theta}_1^n} - \frac{\left(\boldsymbol{\theta}_1^n\right)^H \mathbf{V}_1 \boldsymbol{\theta}_1}{\left(\left(\boldsymbol{\theta}_1^n\right)^H \mathbf{V}_2 \boldsymbol{\theta}_1^n\right)^2} \boldsymbol{\theta}_1^H \mathbf{V}_2 \boldsymbol{\theta}_1 \geq f\left(\boldsymbol{\theta}_1 \left| \boldsymbol{\theta}_1^n \right.\right) + \left[g\left(\boldsymbol{\theta}_1\right) - f\left(\boldsymbol{\theta}_1^n \left| \boldsymbol{\theta}_1^n \right.\right)\right], \tag{20}$$

where the second inequality applies [33, Lemma 2].

With Lemma 2, Eq. (9) that needs to be solved is the maximization of $f(\boldsymbol{\theta}_1|\boldsymbol{\theta}_1^n)$ in Eq. (20) w.r.t $\boldsymbol{\theta}_1$, since $\boldsymbol{\theta}_1^H \mathbf{V}_1 \boldsymbol{\theta}_1$ is a constant.

Thus, the phase shift optimization in each iteration of the MM method is equivalent to

$$\mathcal{P}_0 : \boldsymbol{\theta}_1^{n+1} = \arg\max_{|\boldsymbol{\theta}_1|_m = 1} \Re\left\{\mathbf{v}^H \boldsymbol{\theta}_1\right\}, \tag{21}$$

where $\mathbf{v} = \frac{\mathbf{V}_1\boldsymbol{\theta}_1^n}{(\boldsymbol{\theta}_1^n)^H\mathbf{V}_2\boldsymbol{\theta}_1^n} - \frac{(\boldsymbol{\theta}_1^n)^H\mathbf{V}_1\boldsymbol{\theta}_1^n}{((\boldsymbol{\theta}_1^n)^H\mathbf{V}_2\boldsymbol{\theta}_1^n)^2}$.

From the conclusion in [33], the optimal solution of $\mathcal{P}_0$ is given by $\angle\boldsymbol{\theta}_1 = \angle\mathbf{v}$. Thus, we complete the MM method.

3.4. Summarize of the Proposed Method

To this end, we have solved the problem w.r.t to $\boldsymbol{\theta}_1$. In fact, with fixed $\boldsymbol{\theta}_1$, we can formulate the following problem w.r.t $\boldsymbol{\theta}_2$,

$$\min \quad \frac{\boldsymbol{\theta}_2^H\mathbf{V}_3\boldsymbol{\theta}_2}{\boldsymbol{\theta}_2^H\mathbf{V}_4\boldsymbol{\theta}_2} \tag{22a}$$

$$\text{s.t.} \quad |\boldsymbol{\theta}_2|_m = 1, \tag{22b}$$

where $\mathbf{V}_3 = \mathbf{D}\boldsymbol{\Phi}_1^H\mathbf{F}\mathbf{W}\mathbf{F}^H\boldsymbol{\Phi}_1\mathbf{D}^H \odot (\mathbf{g}_b\mathbf{g}_b^H)^T + \sigma_b^2\mathbf{I}$, and $\mathbf{V}_4 = \mathbf{D}\boldsymbol{\Phi}_1^H\mathbf{F}\mathbf{W}\mathbf{F}^H\boldsymbol{\Phi}_1\mathbf{D}^H \odot (\mathbf{g}_e\mathbf{g}_e^H)^T + \sigma_e^2\mathbf{I}$, respectively.

It is easy to know that the previous ADMM or MM method can be applied to Eq. (22) directly, thus we omit the detail for brevity.

Therefore, we have solved the joint BF design by the AO method, where the active BF can be obtained in a closed form, and the passive BF can be solved using the ADMM or MM method. The entailed AO procedure is summarized in Algorithm 2, where $\{\mathbf{w}^i, \boldsymbol{\theta}_1^i, \boldsymbol{\theta}_2^i\}$ is the obtained optimal solution in the i-th iteration.

Algorithm 2 : The AO method for the joint BF design Eq. (4).

1: **Initialization:** Set $i = 0$, P_s, $\mathbf{F}$, $\mathbf{D}$, $\mathbf{g}_b$, $\mathbf{g}_e$ and the initial $\{\mathbf{w}^0, \boldsymbol{\theta}_1^0, \boldsymbol{\theta}_2^0\}$.
2: **repeat**
[a)]
(i) Calculate $\mathbf{w}^i$ by $\mathbf{w}^i = \sqrt{P_s}\mathbf{v}_{\max}(\mathbf{A}, \mathbf{B})$.
(ii) Calculate $\boldsymbol{\theta}_1^i$ and $\boldsymbol{\theta}_2^i$ by the ADMM or MM method.
(iii) Update $\mathbf{A}$ and $\mathbf{B}$.
(iv) $i \leftarrow i + 1$.
3: **until** the stopping criterion is met.
4: **Output** $\{\mathbf{w}^\star, \boldsymbol{\theta}_1^\star, \boldsymbol{\theta}_2^\star\}$.

3.5. The Complexity Comparison

In this subsection, we analyze the complexity of the ADMM and MM methods and compare them with several other methods. For the convenience of the following statement, we denote $M = \min\{M_1, M_2\}$.

Firstly, for the ADMM method, according to [32], the complexity is $\mathcal{O}(T_{ADMM}M^2 + M^3)$, where T_{ADMM} is the ADMM iteration numbers. On the other hand, for the MM method, according to [11], the complexity is $\mathcal{O}(T_{MM}M^2)$, where T_{MM} is the MM iteration numbers.

In fact, the semi-definite programming (SDP) combining Gaussian randomization (GR) method can be used to solve Eq. (4). However, for the SDP and GR methods, the complexity of the SDP is $O(\sqrt{2}(M+1)^{0.5}M(3M^3+2M^2+M)) \approx O(3\sqrt{2}M^{4.5})$, while the GR with the calculation of the singular value decomposition of $\boldsymbol{\theta}_1\boldsymbol{\theta}_1^H$ and $\boldsymbol{\theta}_2\boldsymbol{\theta}_2^H$ has the complexity of $\mathcal{O}(M^3)$ [13].

From the above comparison, we can see that the SDP and GR methods may lead to higher complexity than the ADMM and MM methods, since T_{ADMM} and T_{MM} are commonly smaller than $3\sqrt{2}M^{2.5}$, especially for large M. In the simulation part, we will compare the converge rate and secrecy performance of these methods.

4. EXTENSION TO OTHER SCENARIOS

4.1. Extension to the Discrete Phase Shifter Case

In the previous part, we focus on the continuous phase shifter case. In fact, we can apply the obtained $\theta_m \in \mathcal{F}_1$, i.e., the solution of Eq. (4), into the discrete phase shifter case $\theta_m \in \mathcal{F}_2$ directly. Specifically, taking $\boldsymbol{\theta}_1$ for example, we denote the solution of $\theta_m \in \mathcal{F}_1$ and $\theta_m \in \mathcal{F}_2$ as $\theta_m^{(1)}$ and $\theta_m^{(2)}$, respectively. Then, we project $\theta_m^{(1)}$ into $\mathcal{F}_2$ to obtain $\theta_m^{(2)}$, i.e.,

$$\theta_m^{(2)} = e^{j\phi_{q^\star}}, \text{ where } q^\star = \arg\min_{1\le q\le \tau} \left|\theta_m^{(1)} - e^{j\phi_q}\right|. \tag{23}$$

The remaining procedure to update $\{\mathbf{w}, \boldsymbol{\theta}_2\}$ is similar to that in the previous part, thus is omitted for brevity.

4.2. Extension to the Multiple IRSs Scenario

Let us assume that the system has L IRSs, each of which has M_l reflection elements, and the phase shift matrix of the l-th IRS is denoted as $\boldsymbol{\Phi}_i$. In addition, we denote the channels between the l-th IRS and the $l+1$-th IRS as $\mathbf{D}_i$.

Then, the received signals at the Bob and Eve can be, respectively, written as

$$y_b = \mathbf{g}_b^H \prod_{i=1}^{L} \mathbf{D}_i \boldsymbol{\Phi}_i^H \mathbf{F}\mathbf{w}s + n_b, \tag{24a}$$

$$y_e = \mathbf{g}_e^H \prod_{i=1}^{L} \mathbf{D}_i \boldsymbol{\Phi}_i^H \mathbf{F}\mathbf{w}s + n_e, \tag{24b}$$

Thus, the previous method can be applied to the multiple IRSs scenario directly, i.e., we optimize the specified $\boldsymbol{\Phi}_i$ when fixing the others.

5. SIMULATIONS RESULTS

In this section, we provide some numerical results to testify the performance of the proposed scheme. The simulation scenario is shown in Fig. 2, where the coordinates of these nodes are (0,0), (10,20), (100,20), (110,0), and (90,0), respectively.

Unless otherwise specified, the simulation settings are assumed as follows: $N = 5$, $M_1 = M_2 = M = 40$, $\tau = 32$, $P_s = 0\,\text{dBW}$, $\sigma_b^2 = \sigma_e^2 = 10^{-8}$. The large-scale path loss is modeled as $L = L_0(d/d_0)^{-\beta}$,

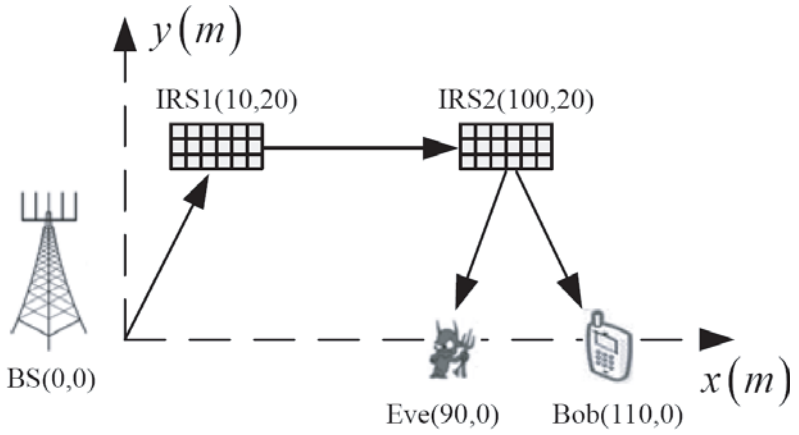

Figure 2. The double IRS-aided secrecy communication scenario.

where $L_0 = 10^{-3}$ is the channel gain at the reference distance $d_0 = 1$, and β denotes the path loss exponent. We set the same path loss exponents $\beta = 3$ for all the IRS-related links. In addition, we assume that the BS-IRS link and IRS-IRS link follow the Rician fading, while the IRS-Bob/Eve links follow the Rayleigh fading.

Firstly, we investigate the convergence behaviour of the proposed AO algorithm. Both the outer layer iteration and inner layer iteration are considered. Specifically, the entire AO algorithm is termed as the outer layer iteration, while the procedure of the ADMM or MM algorithm is termed as the inner layer iterations.

Figure 3 shows the convergence behaviour of the ADMM or MM algorithm for different phase shift numbers. From Fig. 3, we can see that the secrecy rate increases with the iteration numbers for the two methods, and gradually reaches the converge value. Moreover, high secrecy rate can be achieved by using more IRS elements. However, larger M leads to slower convergence, since more variables need to be optimized. Besides, given the same channel condition, the ADMM method can achieve higher secrecy rate than the MM method at the cost of slower converge speed.

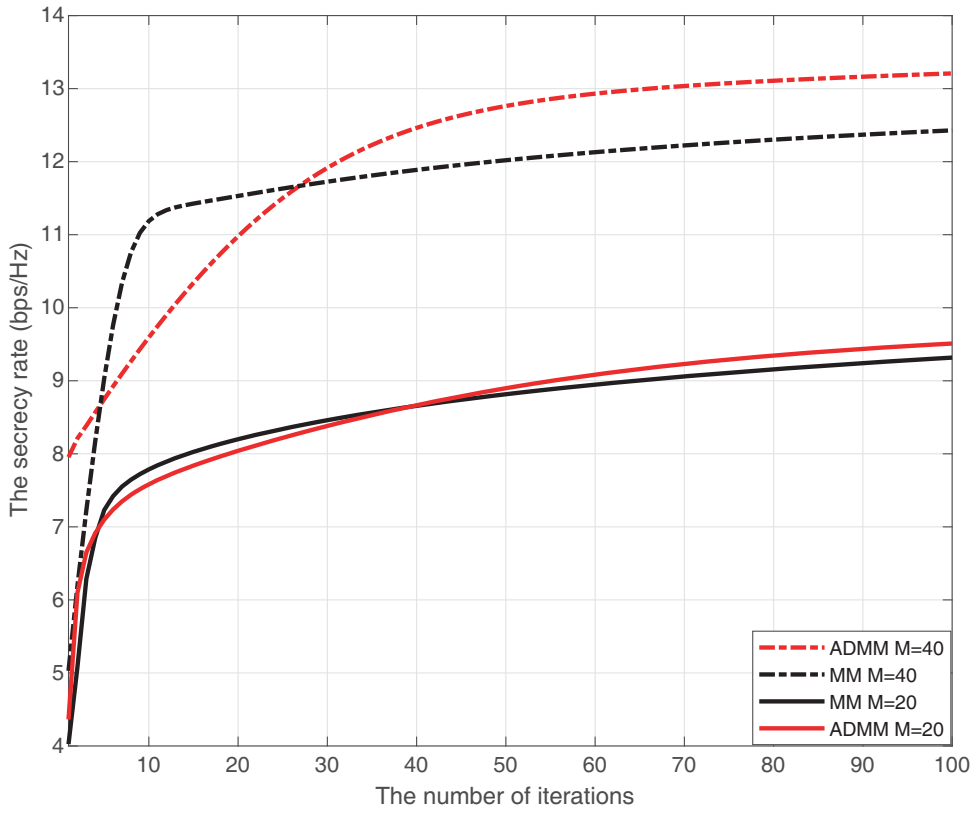

Figure 3. Convergence behaviour of the inner layer iteration.

Now, we investigate the convergence behaviour of the outer AO algorithm. Both the AO-ADMM and AO-MM algorithms are tested. Fig. 4 shows the secrecy rate versus the number of iterations with different M. It can be seen from Fig. 4 that for different values of M, both the AO-ADMM and AO-MM algorithms always converge within 20 iterations, which confirms the practicality of the proposed design. Besides, given the same channel condition, the two methods have a similar converge speed, while the AO-ADMM method can achieve higher secrecy rate than the AO-MM method.

In the following, we will show the algorithm performance against several system parameters. Both the ADMM and MM methods are considered in the scenario of continuous and discrete RC cases. In addition, we compare our designs with the following methods: 1) the element-by-element optimization (EEO) method in [11]; 2) the SDP-GR method in [13]; 3) the AF relay method. These methods

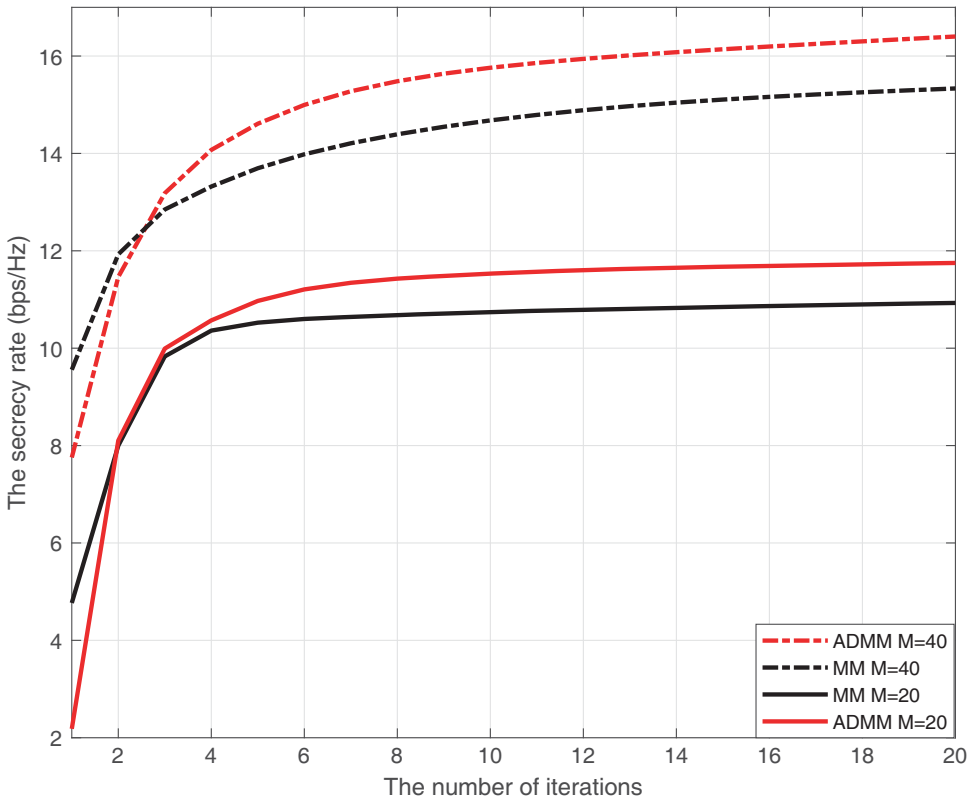

Figure 4. Convergence behaviour of the outer layer iteration.

are labeled as "the continuous RC ADMM", "the continuous RC MM", "the discrete RC ADMM", "the discrete RC MM", "the EEO method", "the SDP-GR method", and "the AF relay method", respectively.

Firstly, we compare the secrecy rate of these schemes versus the transmit power budget P_s, and the result is shown in Fig. 5. From this figure, we can see that with the increase of P_s, the secrecy rate increases for all these methods. The proposed continuous RC ADMM method obtains the best performance among the IRS-aided methods. Besides, we can find that the security gain obtained by the proposed scheme is greater than the SDR-GR method. This is because the phase shifts of the IRS are properly designed, not chosen randomly. This comparison shows that optimizing the phase shifts is important. Furthermore, for the AF relay method, when the transmission power is relatively low, the AF relay achieves better performance than the IRS-aided methods. However, when the transmission power becomes large, the IRS-aided methods with properly designed phase matrix outperform the AF relay method, since in this case, the magnification time of the relay is limited, and the noise at the relay becomes the main performance bottleneck of the network.

Lastly, we show the secrecy rate of these schemes versus the number of reflecting elements M in Fig. 6. From Fig. 6, we can see that the secrecy rate increases with the increase of M. This is mainly due to two reasons. On the one hand, a higher array gain can be obtained by increasing M, since more signals can be reached at the IRS. On the other hand, a higher reflecting BF gain can be obtained by increasing M, since the sum of the reflected signals at the IRS increases with M by appropriately designing the phase shifts. These results show that more security improvement can be obtained by using a large IRS and optimizing the phase shifts properly.

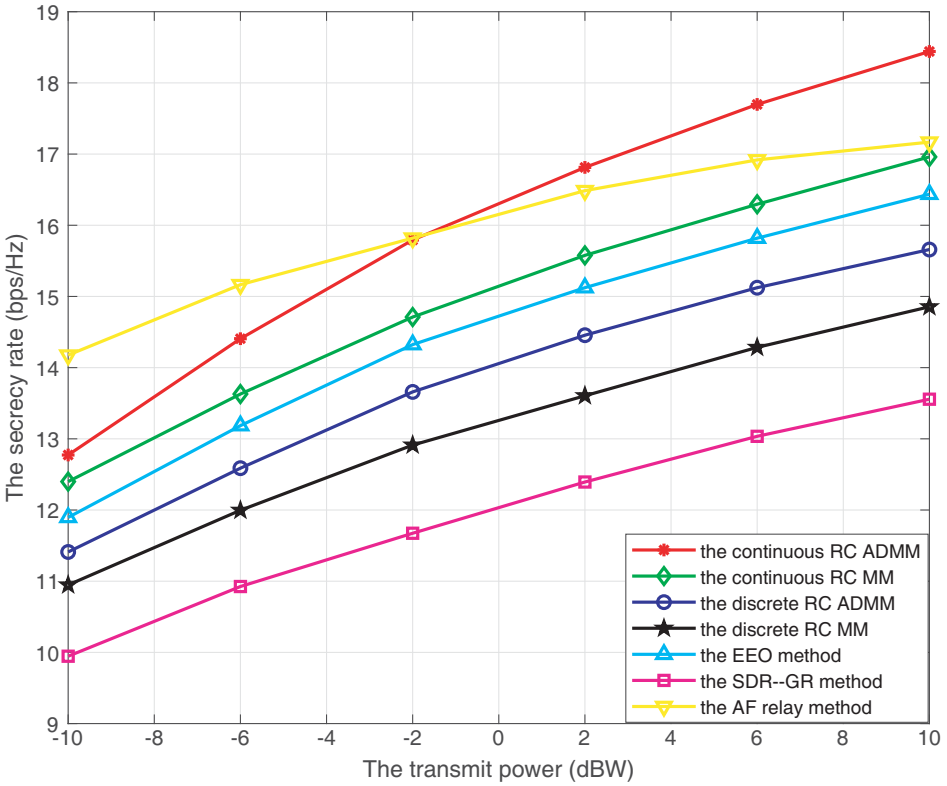

Figure 5. The secrecy rate versus the transmit power budget.

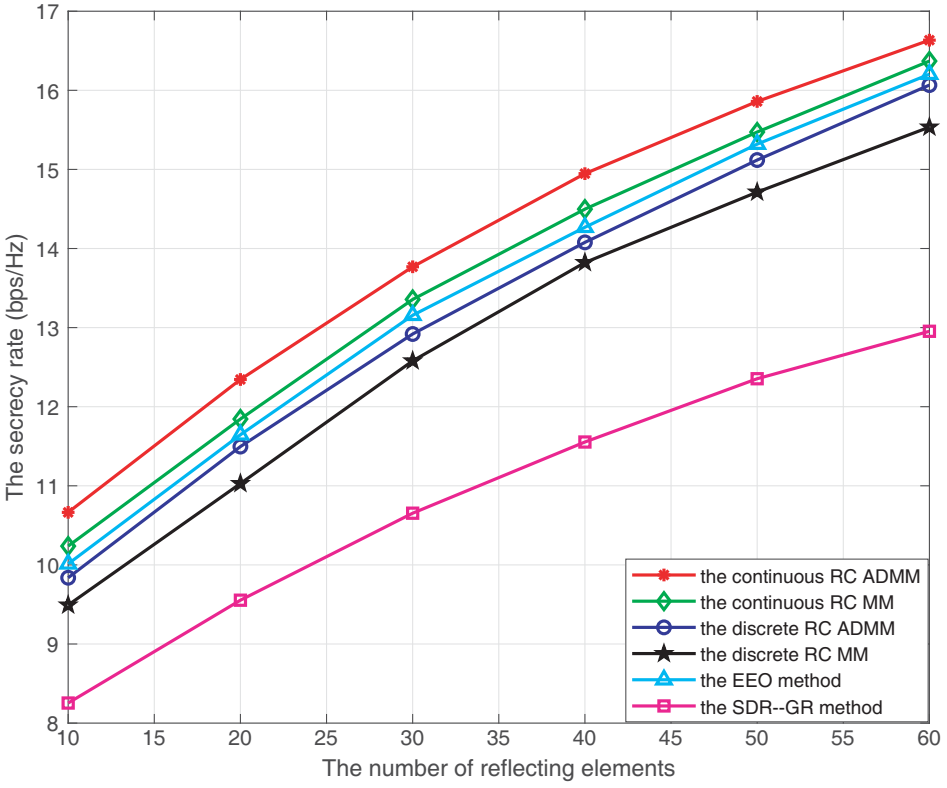

Figure 6. The secrecy rate versus the number of reflecting elements.

6. CONCLUSIONS

In this paper, we have studied the double IRS aided secrecy transmission in a MISO wiretap channel. Specifically, we aimed to maximize the secrecy rate by jointly optimizing the BF vector and the two phase shifts at the IRSs, subject to the transmission power constraint and the UMC. To solve the formulated non-convex problem, we utilized the ADMM and MM methods to handle the UMC, then an AO algorithm was proposed. Simulation result demonstrated the performance of the proposed design.

ACKNOWLEDGMENT

This work was supported by the Industry-University-Research Cooperation Project of Jiangsu Province under Grant No. BY2018282.

REFERENCES

1. Donelli, M. and P. Febvre, "An inexpensive reconfigurable planar array for Wi-Fi applications," *Progress In Electromagnetics Research C*, Vol. 28, 71–81, 2012.
2. Donelli, M., T. Moriyama, and M. Manekiya, "A compact switched-beam planar antenna array for wireless sensors operating at Wi-Fi band," *Progress In Electromagnetics Research C*, Vol. 83, 137–145, 2018.
3. Rocca, P., M. Donelli, G. Oliveri, F. Viani, and A. Massa, "Reconfigurable sum-difference pattern by means of parasitic elements for forward-looking monopulse radar," *IET Radar, Sonar and Navigation*, Vol. 7, No. 7, 747–754, 2013.
4. Hu, S., F. Rusek, and O. Edfors, "Beyond massive MIMO: The potential of data transmission with large intelligent surfaces," *IEEE Trans. Signal Process.*, Vol. 66, No. 10, 2746–2758, May 2018.
5. Lyu, J., and R. Zhang, "Spatial throughput characterization for intelligent reflecting surface aided multiuser system," *IEEE Wireless Commun. Lett.*, Vol. 9, No. 6, 834–838, Jun. 2020.
6. Yan, W., X. Yuan, Z.-Q. He, and X. Kuai, "Passive beamforming and information transfer design for reconfigurable intelligent surfaces aided multiuser MIMO systems," *IEEE J. Sel. Areas Commun.*, Vol. 38, No. 8, 1793–1808, Aug. 2020.
7. Tang, W., M. Chen, J. Dai, Y. Zeng, X. Zhao, S. Jin, Q. Cheng, and T. Cui, "Wireless communications with programmable metasurface new paradigms, opportunities, and challenges on transceiver design," *IEEE Wireless Commun.*, Vol. 27, No. 2, 180–187, Apr. 2020.
8. Wu, Q. and R. Zhang, "Towards smart and reconfigurable environment: Intelligent reflecting surface aided wireless networks," *IEEE Commun. Mag.*, Vol. 58, No. 1, 106–112, Jan. 2020.
9. Gong, S., X. Lu, D. Hoang, D. Niyato, L. Shu, D. Kim, and Y. C. Liang, "Towards smart wireless communications via intelligent reflecting surfaces: A contemporary survey," *IEEE Commun. Surveys Tut.*, June 2020.
10. Huang, C., A. Zappone, G. C. Alexandropoulos, M. Debbah, and C. Yuen, "Reconfigurable intelligent surfaces for energy efficiency in wireless communication," *IEEE Trans. Wireless Commun.*, Vol. 18, No. 8, 4157–4170, Aug. 2019.
11. Guo, H., Y. Liang, J. Chen, and E. G. Larsson, "Weighted sum-rate optimization for intelligent reflecting surface enhanced wireless networks," 2019, [Online], available: https://arxiv.org/abs/1905.07920.
12. Cao, Y., T. Lv, Z. Lin, W. Ni, and N. C. Beaulieu, "Delay-constrained joint power control, user detection and passive beamforming in intelligent reflecting surface assisted uplink mmWave system," 2019, [Online], available: https://arxiv.org/abs/1912.10030.
13. Yuan, J., Y. C. Liang, J. Joung, G. Feng, and E. G. Larsson, "Intelligent reflecting surface-assisted cognitive radio system," 2019, [Online], available: https://arxiv.org/abs/1912.10678.
14. Pan, C., H. Ren, K. Wang, M. Elkashlan, A. Nallanathan, J. Wang, and L. Hanzo, "Intelligent reflecting surface aided MIMO broadcasting for simultaneous wireless information and power transfer," *IEEE J. Sel. Areas Commun.*, Vol. 38, No. 8, 1719–1734, Aug. 2020.

15. Li, S., B. Duo, X. Yuan, Y. Liang, and M. Renzo, "Reconfigurable intelligent surface assisted UAV communication: Joint trajectory design and passive beamforming," *IEEE Wireless Commun. Lett.*, Vol. 9, No. 5, 716–720, May 2020.
16. Feng, K., Q. Wang, X. Li, and C.-K. Wen, "Deep reinforcement learning based intelligent reflecting surface optimization for MISO communication systems," *IEEE Wireless Commun. Lett.*, Vol. 9, No. 5, 745–749, May 2020.
17. Chen, X., D. W. K. Ng, W. Gerstacker, and H.-H. Chen, "A survey on multiple-antenna techniques for physical layer security," *IEEE Commun. Surveys Tut.*, Vol. 19, No. 2, 1027–1053, 2nd Quart. 2017.
18. Hamamreh, J. M., H. M. Furqan, and H. Arslan, "Classifications and applications of physical layer security techniques for confidentiality: A comprehensive survey," *IEEE Commun. Surveys Tut.*, Vol. 21, No. 2, 1773–1828, 2nd Quart. 2019.
19. Jameel, F., S. Wyne, G. Kaddoum, and T. Q. Duong, "A comprehensive survey on cooperative relaying and jamming strategies for physical layer security," *IEEE Commun. Surveys Tut.*, Vol. 21, No. 3, 2734–2771, 3rd Quart. 2019.
20. Chu, Z., W. Hao, P. Xiao, and J. Shi, "Intelligent reflecting surface aided multi-antenna secure transmission," *IEEE Wireless Commun. Lett.*, Vol. 9, No. 1, 108–112, Jan. 2020.
21. Guan, X., Q. Wu, and R. Zhang, "Intelligent reflecting surface assisted secrecy communication: Is artificial noise helpful or not?," *IEEE Wireless Commun. Lett.*, Vol. 9, No. 6, 778–782, Jun. 2020.
22. Wang, H., J. Bai, and L. Dong, "Intelligent reflecting surfaces assisted secure transmission without eavesdropper's CSI," *IEEE Signal Process. Lett.*, Vol. 27, 1300–1304, Jul. 2020.
23. Dong, L. and H. Wang, "Enhancing secure MIMO transmission via intelligent reflecting surface," *IEEE Trans. Wireless Commun.*, Vol. 19, No. 11, 7543–7556, 2020.
24. Dong, L. and H.-M. Wang, "Secure MIMO transmission via intelligent reflecting surface," *IEEE Wireless Commun. Lett.*, Vol. 9, No. 6, 787–790, Jun. 2020.
25. Hong, S., C. Pan, H. Ren, K. Wang, and A. Nallanathan, "Artificial-noise-aided secure MIMO wireless communications via intelligent reflecting surface," *IEEE Trans. Commun.*, Vol. 68, No. 12, 7851–7866, 2020.
26. Niu, H. and L. Ni, "Intelligent reflect surface aided secure transmission in MIMO channel with SWIPT," *IEEE Access*, Vol. 8, 192132–192140, Oct. 2020.
27. Yu, X., D. Xu, Y. Sun, D. W. K. Ng, and R. Schober, "Robust and secure wireless communications via intelligent reflecting surfaces," *IEEE J. Sel. Areas Commun.*, Vol. 38, No. 11, 2637–2652, Nov. 2020.
28. Wang, Q., F. Zhou, R. Q. Hu, and Y. Qian, "Energy efficient robust beamforming and cooperative jamming design for IRS-assisted MISO networks," 2020, [online], avaiable: https://arxiv.org/abs/2012.04843.
29. Han, Y., S. Zhang, L. Duan, and R. Zhang, "Cooperative double-IRS aided communication beamforming design and power scaling," *IEEE Wireless Commun. Lett.*, Vol. 9, No. 8, 1206–1210, Aug. 2020.
30. You, C., B. Zheng, and R. Zhang, "Wireless communication via double IRS: Channel estimation and passive beamforming designs," 2020, [Online], available: https://arxiv.org/abs/2008.11439.
31. Zheng, B., C. You, and R. Zhang, "Double-IRS assisted multi-user MIMO: Cooperative passive beamforming design," 2020, [Online], available: https://arxiv.org/abs/2009.13701.
32. Fan, W., J. Liang, and J. Li, "Constant modulus MIMO radar waveform design with minimum peak sidelobe transmit beampattern," *IEEE Trans. Signal Process.*, Vol. 66, No. 16, 4207–4222, Aug. 2018.
33. Yu, X., D. Xu, and R. Schober, "Enabling secure wireless communications via intelligent reflecting surfaces," *Proc. IEEE Global Commun. Conf.*, 1–6, Waikoloa, HI, USA, Dec. 2019.